Diurnal Tidal Motions Near the Stratopause during 48 Hours at White Sands Missile Range

N. J. BEYERS AND B. T. MIERS

U. S. Army Electronics Research and Development Activity, White Sands Missile Range, N. Mex.

AND R. J. REED

University of Washington, Seatile

(Manuscript received 28 December 1965)

ABSTRACT

Wind and temperature soundings from a series of 16 meteorological rocket firings over a period of 51 hours between 30 June and 2 July 1965 are presented. Harmonic analysis revealed large diurnal oscillations in the zonal and meridional winds. Both components displayed amplitudes of about 12 m sec^{-1} near the stratopause (52–56 km) with the phase of the meridional (v) component leading the zonal (u) component by about 5–7 hours at that level. The v component was generally more uniform in both phase and amplitude over the two-day period. Harmonic analysis of the temperatures also revealed a diurnal oscillation with an amplitude of 8.2C at 52 km with the maximum occurring near 1330 hours local time. An attempt to arrive at an independent estimate of the temperature cycle, based essentially on a generalized thermal wind equation, yielded inconclusive results. When this series was combined with previous data, it was concluded that an unmistakable, dominant, diurnal tidal oscillation exists in the stratopause region over White Sands Missile Range (32N) during most or all seasons, particularly in the meridional component.

1. Introduction

Three series of rocket wind soundings have been conducted recently which indicate the existence of pronounced diurnal wind and temperature oscillations near the stratopause (45–50 km). As reported by Lenhard (1963) and Miers (1965), the soundings were taken at regular intervals over a 24-hr period and extended over the altitude range of approximately 30–55 km. Though each series was performed during a different month of the year (February, May and November), the amplitude of the diurnal wind oscillation was uniformly large (5–10 m sec^{-1}) in the region about the stratopause. Amplitudes were considerably smaller (1–3 m sec^{-1}) below 40 km and appeared to decrease slightly above 50 km. The February series also included temperature measurements which revealed a surprisingly large diurnal temperature range of about 15–20C in the stratopause region (Beyers and Miers, 1965).

Because of the limited duration of the three series and the presence of considerable random scatter in the data, it was not possible to determine whether the results of the harmonic analyses were representative of recurring tidal motions. To overcome this deficiency and to test for the existence of similar oscillations during a different season, an experiment was conducted over a two-day period during the summer of 1965 at White Sands Missile Range. The results of this experiment are presented here.

2. Description of the experiment

Starting at 0800 MST 30 June 1965, meteorological rocket soundings were made every six hours for 24 hours concluding at 0800 MST 1 July 1965. Then commencing at 1100 MST 1 July 1965, firings were resumed at 6-hr intervals for 24 hours. All soundings were made with Arcas rockets equipped with 4.6-m parachute wind sensors and Arcasonde 1A temperature measuring systems. In addition, rocket soundings made with Judi rockets equipped with 2.7-m parachutes were spaced halfway between each of the Arcas soundings, resulting in a sounding schedule every three hours for 51 hours. Three of the sounding attempts were unsuccessful, and several other minor deviations in the planned schedule were necessitated. A summary of the successful soundings is presented in Table 1.

Basic data for determination of wind profiles consisted of the time-position output of AN/FPS-16A Instrumentation Radar recordings at ten points per second. The radar output was programmed on an IBM 7044 electronic computer to convert the horizontal motion of the parachute as it descended into a "true" wind profile. The program incorporated a technique developed by Eddy *et al.* (1965) designed to filter out radar tracking noise and deduce the "true" wind from the damped or smoothed horizontal motion of the parachute.

TABLE 1. Firing schedule for series of meteorological rockets during period between 30 June–2 July 1965 at White Sands Missile Range.

Date	Time (MST)	Date	Time (MST)	Date	Time (MST)
30 June 1965	0805(A)	1 July 1965	0200(A)*	2 July 1965	0500(A)
	1110(J)		0800(A)*		0530(A)
	1400(A)*		1112(A)*		0800(A)
	1705(J)		1530 (J)		1100(A)*
	2000(A)*		1705(A)*		
			2000(J)		
			2300(A)*		

(A) = Arcas; (J) = Judi; asterisks indicate temperature soundings.

3. Results

The results of the wind soundings are presented in the time sections of Figs. 1a and 1b. Here we have averaged the zonal and meridional components over 4-km layers centered at the levels in the figures. The behavior of the meridional (v) component (Fig. 1a) is particularly striking. Among the most notable features are the consistent sinusoidal appearance between 44 and 56 km with a period of 24 hr, and the general increase in amplitude and regular shift in phase with altitude. While the behavior of the wind component is similar on both days in the layer from 44 to 56 km, it is less regular at 60 km with the second day fitting better with the pattern at lower layers. The 40-km level displays a somewhat irregular wave motion with varying period and small amplitude. It is also interesting to note that at all levels the meridional component oscillates very nearly about zero velocity.

The zonal wind (u) behavior (Fig. 1b) is less uniform, though there are clear indications of a recurrent diurnal wave with approximately the same amplitude as the meridional oscillation. Again the most consistent patterns occur at the 44-, 48-, 52- and 56-km levels. The pattern at 60 km seems somewhat disorganized on the first day, while better fitting the picture at lower layers on the second day. At the 40-km level the oscillation is again weak and irregular. The zonal component oscillates about a mean easterly flow ranging between 30–60 m sec^{-1}, as indicated in Fig. 1b. In both figures only the diurnal period (or first harmonic) is readily discernible at the majority of levels.

A harmonic analysis was performed on the wind data following the standard technique described by Conrad and Pollak (1950). Only the 6-hr Arcas soundings were used in the analysis. There were two reasons for this procedure: 1) successful Arcas soundings were obtained every six hours while some Judi soundings

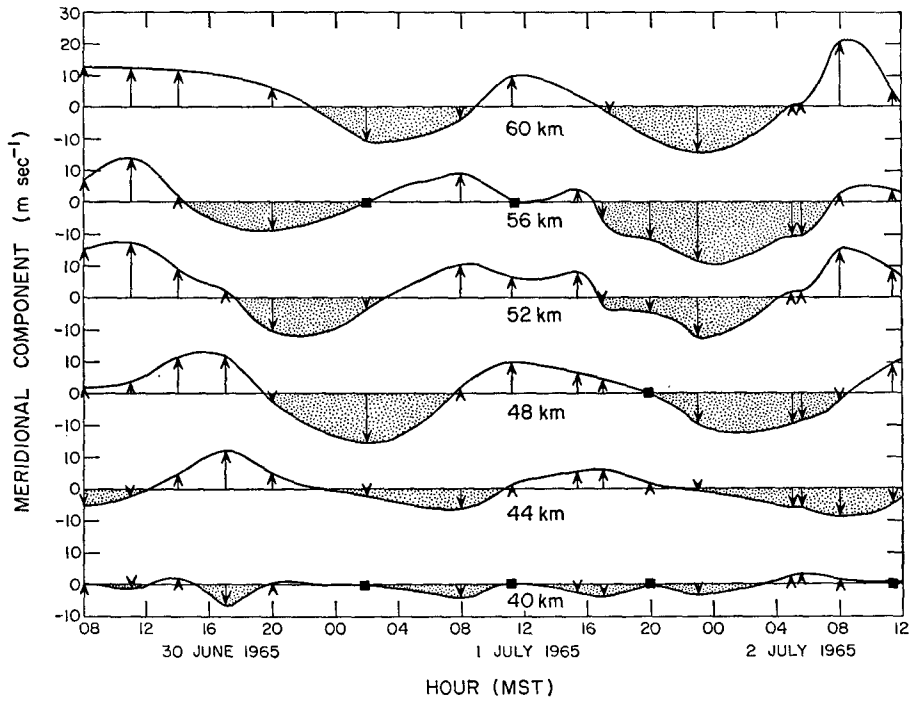

FIG. 1a. Meridional wind components in m sec^{-1} averaged over 4-km layers centered at 40, 44, 48, 52, 56 and 60 km. Positive values indicate a south to north flow.

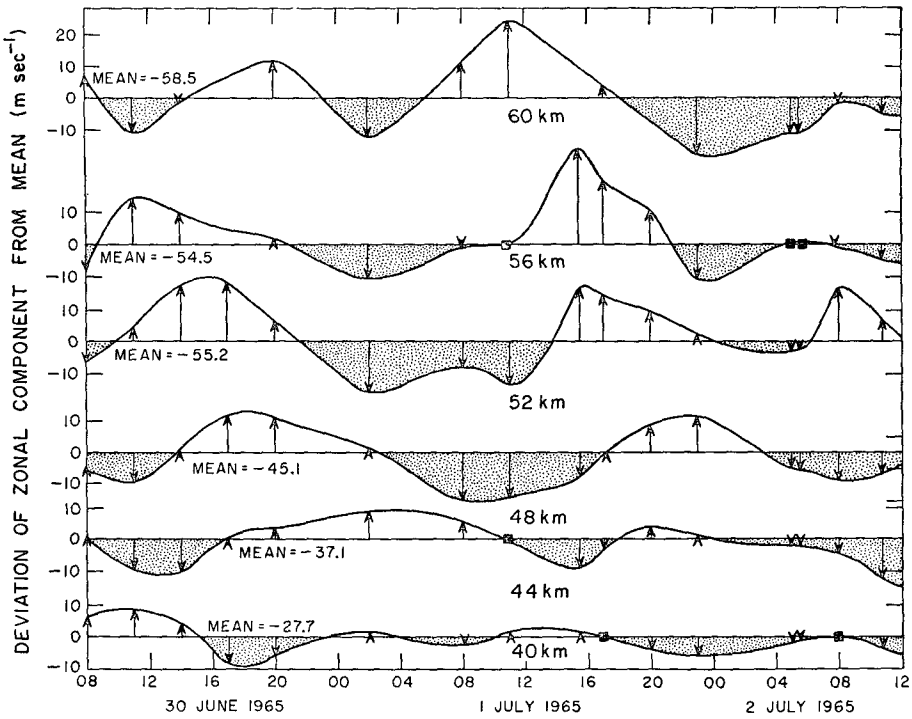

FIG. 1b. Zonal wind components in m sec^{-1} averaged over 4-km layers centered at 40, 44, 48, 52, 56 and 60 km. Oscillation about the 48-hr mean indicates the maximum and minimum values of the east to west flow.

failed, and 2) the Arcas system gave good data to higher altitudes than the Judi system with its smaller parachute and higher fall velocity in the stratopause region. Consequently, the soundings of 0805, 1400, and 2000 MST 30 June 1965 and 2000 MST 1 July 1965 were used in the harmonic analysis for the first day

TABLE 2a. Results of harmonic analysis of meridional (v) wind components. a and b are coefficients, A the amplitude (m sec^{-1}), α the phase angle (deg) of the starting time with respect to the upcrossing through the zero point. Starting times were: (1st day) 0800 MST; (2nd day) 1100 MST; (1st & 2nd day) 0800 MST. t_m is the time of maximum (hours, MST).

	Diurnal									
Alt	1st day					2nd day				
(km)	a	b	A	α	t_m	a	b	A	α	t_m
40	−0.6	0.6	0.8	196	16.9	1.9	−2.9	3.5	342	7.2
44	−5.2	3.1	6.1	181	17.9	1.0	6.1	6.1	204	16.4
48	2.0	13.8	13.9	248	13.5	9.7	6.8	11.8	250	13.3
52	13.0	6.2	14.4	305	9.7	9.1	−2.4	9.4	300	10.0
56	7.6	1.0	7.6	323	8.5	9.8	2.1	10.0	273	11.8
60	3.6	11.4	11.9	257	12.9	12.2	−1.4	12.3	291	10.6

	1st and 2nd day				
Alt (km)	a	b	A	α	t_m
40	1·4	−0.1	1.4	333	7.8
44	−4.4	4.1	6.0	193	17.1
48	2.0	12.7	12.9	249	13.4
52	10.6	5.5	11.9	303	9.8
56	6.5	4.7	8.0	294	10.4
60	6.6	9.5	11.6	275	11.7

	Semidiurnal					Terdiurnal				
Alt (km)	a	b	A	α	t_m	a	b	A	α	t_m
40	−0.1	−0.2	0.3	89	4.0	−2.0	−0.7	2.1	132	4.4
44	−0.5	0.1	0.5	164	1.5	−0.8	0.9	1.2	199	3.0
48	0.7	1.2	1.4	270	10.0	0	−1.1	1.1	62	6.0
52	−0.4	−1.4	1.5	77	4.4	2.4	−0.7	2.5	347	7.6
56	−0.8	0	0.8	149	2.0	1.1	3.7	3.9	256	1.6
60	4.6	−1.0	4.7	342	7.6	−3.0	−1.9	3.5	118	4.7

TABLE 2b. Same as Table 2a except pertaining to zonal (u) components.

Alt (km)	Diurnal 1st day a	b	A	α	t_m	Diurnal 2nd day a	b	A	α	t_m
40	6.0	1.2	6.1	319	8.6	3.5	0.9	3.6	271	11.9
44	−1.0	−10.0	9.7	66	1.6	−1.1	−0.5	1.2	79	0.7
58	−8.7	0	8.7	150	20.0	−12.9	2.6	13.2	116	22.3
52	−6.0	17.3	18.3	221	15.3	−8.0	8.6	11.7	152	19.9
56	−5.5	10.2	11.6	212	15.9	5.6	9.4	10.9	226	14.9
60	−2.7	5.3	6.0	213	15.8	20.9	7.2	22.0	266	12.3

Alt (km)	1st and 2nd day a	b	A	α	t_m
40	3.9	2.1	4.5	302	9.9
44	−0.7	−5.4	5.4	67	1.5
48	−9.8	−3.7	10.5	130	21.3
52	−8.9	8.9	12.5	195	17.5
56	−4.1	10.4	11.2	218	15.5
60	3.5	12.6	13.0	256	12.9

Alt (km)	Semidiurnal a	b	A	α	t_m	Terdiurnal a	b	A	α	t_m
40	−1.3	−0.6	1.4	5	2.8	2.1	1.0	2.3	305	0.6
44	1.7	1.6	2.3	288	9.4	−0.3	4.2	4.2	236	2.1
48	0.4	0.8	0.9	269	10.0	1.2	−3.6	3.8	52	6.4
52	−0.9	−5.6	5.7	69	4.7	2.9	−8.4	8.9	51	6.4
56	−1.3	−8.0	8.1	69	4.7	−1.4	0.2	1.4	159	3.8
60	7.7	3.6	8.5	305	8.8	−6.2	7.3	9.5	199	2.9

and the soundings of 1112, 1705 and 2300 MST 1 July 1965 and 0500 MST 2 July 1965 for the second day. The results of the analysis are found in Tables 2a and 2b. A further harmonic analysis was made by combining the above soundings into one 24-hr period,

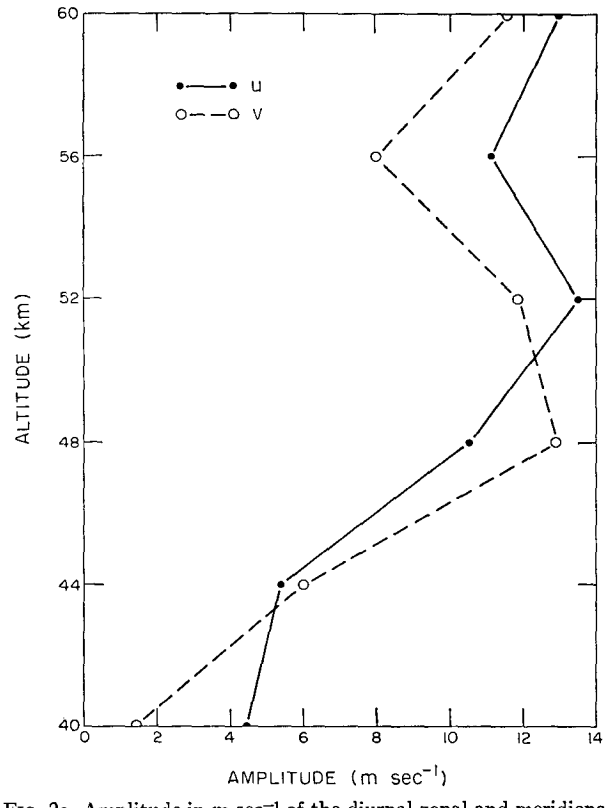

FIG. 2a. Amplitude in m sec^{-1} of the diurnal zonal and meridional wind components as determined from harmonic analysis.

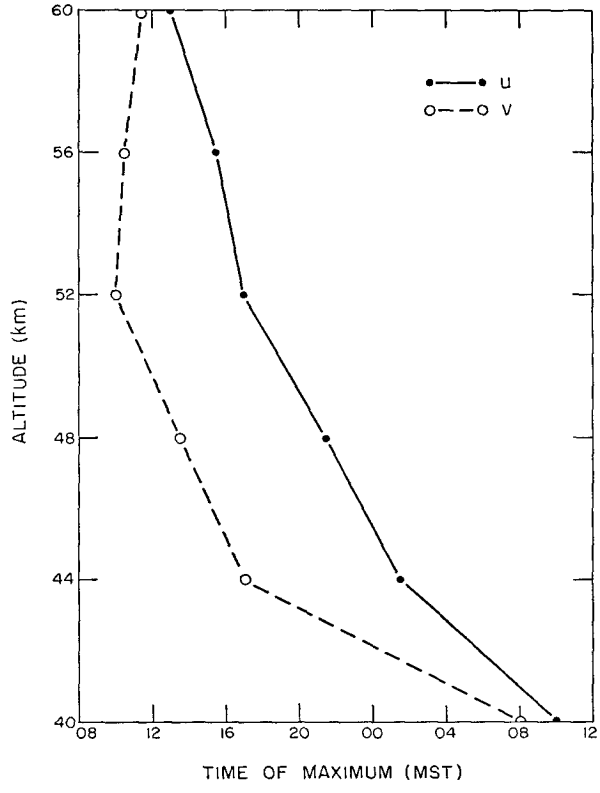

FIG. 2b. Time of maximum of the diurnal zonal and meridional wind components as determined from harmonic analysis. Time is local standard.

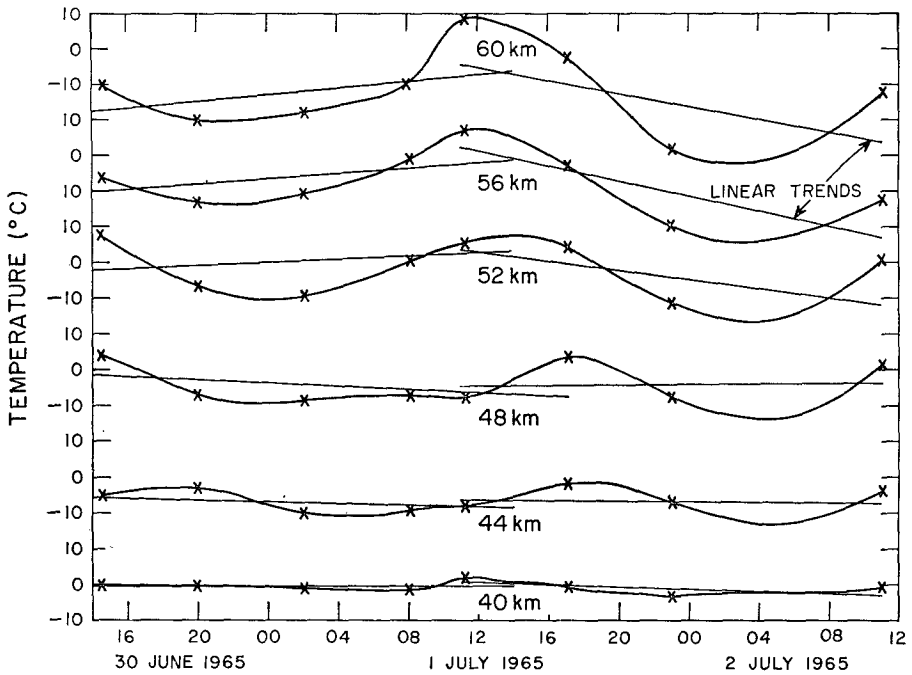

FIG. 3. Temperature values (°C) averaged over 4-km layers centered at 40, 44, 48, 52, 56 and 60 km. A smooth curve was drawn through the points and a linear trend for each day was computed and shown by the straight sloping lines.

thereby generating data points every three hours. With data available at three hour intervals it was then possible to compute the second and third harmonics. These are included in Tables 2a and 2b, though it is believed from their erratic behavior that they do not represent real variations. The amplitudes and phases (local times of occurrence of maxima) of the diurnal component for the combined days are presented in Figs. 2a and 2b. Both components have similar profiles with increasing amplitudes from 40 km to the stratopause region, where peak values of 10–12 m sec^{-1} are observed, then decreasing amplitudes up to 56 km, and finally increasing amplitudes again to 60 km. The phase difference between the zonal and meridional wind variation is 7–8 hr between 44 and 56 km, and 1–2 hr at both 40 and 60 km. The two-day combination reduces the inconsistency at the 60-km level so that the regular phase shift with altitude extends through that level.

Eight of the Arcas soundings yielded temperature recordings as indicated in Table 1. Consistent with the processing of the data, the temperatures presented in Fig. 3 were averaged over 4-km layers. There appears to be a large diurnal oscillation in these data, and also a relatively large synoptic trend. The trend was computed by a least squares technique and is included in the time section of Fig. 3. It amounts to the large figure of 25C per 24 hr at 56 km during the second day. It essentially disappears at 48 km.

The temperature data were subjected to harmonic analysis after the trend was removed and the points for the two days were combined as in the analysis of the wind data. It was necessary to interpolate a value for 0500 MST from the values at 0200 and 0800 MST. The results of the harmonic analysis are summarized in Table 3a and Fig. 4.

The amplitude of the temperature oscillation increases from less than 2.0C at 40 km to 5.5C at 48 km and averages 7.5C up to 56 km with a sharp increase

TABLE 3a. Results of harmonic analysis of temperature data obtained from 30 June–2 July 1965 series of meteorological rocket soundings at White Sands Missile Range. a and b are coefficients, A the amplitude (m sec^{-1}), α the phase angle (degrees) of the starting time with respect to the upcrossing through the zero point. The starting time is 1100 MST. t_m is the time of maximum (hours, MST).

Alt	Diurnal					Semidiurnal				
(km)	a	b	A	α	t_m	a	b	A	α	t_m
40	0.9	1.1	1.4	39	14.4	0.4	0.2	0.4	68	11.7
44	−0.3	3.5	3.6	355	17.3	−0.5	−0.8	1.0	214	18.9
48	2.3	5.0	5.5	25	15.3	−2.0	1.8	2.7	311	15.6
52	6.4	5.2	8.2	51	13.6	−0.8	1.8	2.0	336	14.8
56	7.0	2.6	7.4	70	12.3	0.2	0.7	0.7	15	13.5
60	9.4	2.7	9.8	74	12.1	2.0	2.1	2.9	43	12.6

TABLE 3b. Same as Table 3a except for data on 7–8 February 1964 at White Sands. Starting time was 0400 MST.

Alt (km)	Diurnal					Semidiurnal				
	a	b	A	α	t_m	a	b	A	α	t_m
40	−1.1	1.7	2.0	326	12.3	−0.9	−1.0	1.3	123	11.6
44	−1.4	0.9	1.6	303	13.8	−2.5	−0.8	2.7	153	10.6
48	−5.2	3.3	6.2	303	13.8	−0.4	−0.7	0.9	210	12.0
52	−4.8	4.2	6.4	311	13.3	−2.1	−2.5	3.2	220	11.7
55	−5.6	4.5	7.2	309	13.4	−2.9	−1.5	3.2	243	10.9

above 56 km. The time of maximum shows a consistent trend from 44 km upward varying from 1715 MST at that level to 1200 MST at 60 km. The time of maximum (at 40 km) may not be representative since the amplitude is near the threshold of the noise (random error) level.

For comparative purposes, data from the February 1964 series (Beyers and Miers, 1965) are included in Fig. 4 and Table 3b. The two series seem to be in good agreement in both phase and amplitude above 44 km.

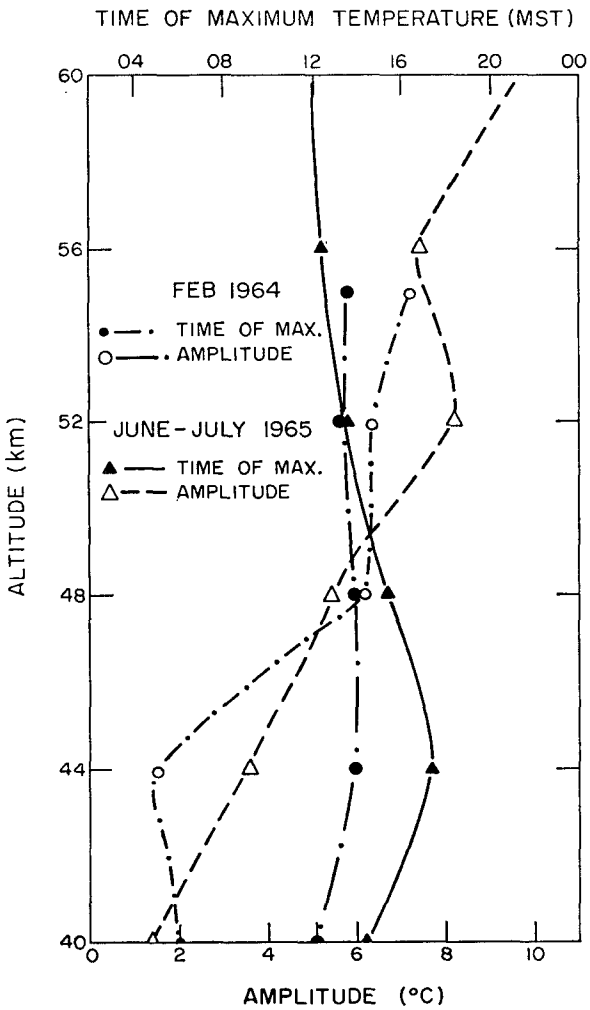

FIG. 4. Amplitude (lower scale) of the summer 1965 and February 1964 temperature oscillation (°C) and the time of maximum temperature (upper scale) as determined from harmonic analysis. Time is local standard.

4. Compatibility of the wind and temperature results

It is possible in theory to check the compatibility of the observed wind and temperature oscillations by use of a method employed previously by Harris *et al.* (1962) in studying tidal motions over the Azores. The wide discrepancy between the observed diurnal temperature variation and the variation predicted theoretically by Leovy (1964)[1] and others (Johnson, 1953; Pressman, 1955) from radiative considerations (see Table 4) raises questions concerning the accuracy of the temperature measurements and makes it desirable to verify them by independent means, if possible. In brief, the method involves substituting the observed wind components in the east-west equation of motion to obtain geopotential height variations at several pressure levels, subtracting the heights to get thickness variations between the pressure levels, and applying the hydrostatic equation to convert thickness variations to mean temperature variations.

If u and v represent the perturbed wind components in the x(east) and y(north) directions and h the geopotential height perturbation, the equation of motion in the x-direction may be written

$$\frac{\partial u}{\partial t}-fv=-g\frac{\partial h}{\partial x}, \tag{1}$$

where f is the coriolis parameter and g is the acceleration of gravity.

Assuming now propagating wave components of the form

$$\begin{bmatrix} u \\ v \\ h \end{bmatrix}=\begin{bmatrix} \hat{U} \\ \hat{V} \\ \hat{H} \end{bmatrix}e^{i(\nu t+\eta x)}, \tag{2}$$

where $\hat{U}$, $\hat{V}$, $\hat{H}$ are the complex amplitudes of u, v and h, respectively, i is the unit imaginary, ν is the frequency (2π day^{-1}) and η is the wave number (2π/circumference of latitude circle), we obtain the following expression for h in terms of u and v:

$$h=-(g\eta)^{-1}(\nu u+ifv). \tag{3}$$

[1] Also, personal communication, 1965.

TABLE 4. Comparison of observed temperatures, theoretical temperatures (Leovy, 1964)* and temperatures computed from wind observations. Phase gives time of maximum.

Height (km)	Observed temperatures Amplitude (°C)	Observed temperatures Phase (hr)	Theoretical temperatures Amplitude (°C)	Theoretical temperatures Phase (hr)	Computed geopotential heights Amplitude (m)	Computed geopotential heights Phase (hr)	Computed temperatures Amplitude (°C)	Computed temperatures Phase (hr)
40	1.4	14.4	1.8	~18.0	153	20.5		
							3.2	13.9
44	3.6	17.3	2.1	~18.0	153	19.3		
							13.6	13.8
48	5.5	15.3	2.2	~18.0	261	16.2		
							18.1	6.4
52	8.2	13.6	2.1	~18.0	153	10.7		
							18.9	23.6
56	7.4	12.3	2.0	~18.0	136	0.3		
							31.6	21.0
60	9.8	12.1	1.8	~18.0	576	21.6		

* Also, personal communication, 1965.

Upon making appropriate trigonometric substitutions, the following expressions are obtained for the amplitude, H, and phase advance, ϕ_h, of the height wave:

$$\left.\begin{aligned} H &= (g\eta)^{-1}[\nu^2U^2+f^2V^2-2\nu fUV\sin(\phi_v-\phi_u)]^{\frac{1}{2}} \\ \phi_h &= \arctan\frac{\nu U\sin\phi_u+fV\cos\phi_v}{\nu U\cos\phi_u-fV\sin\phi_v} \end{aligned}\right\}. \quad (4)$$

In these expressions U, V and H represent real amplitudes and ϕ_u and ϕ_v denote the phase advances of u and v relative to the time origin. Although for strict accuracy wind components at constant pressure should be employed in these equations, little error results if values at constant altitude are used instead.

The remainder of the computation of the temperature perturbation proceeds in a straightforward manner which requires no elaboration. Results of the computation appear in the final columns of Table 4.

Except for the bottom layer, the computed temperature behavior is in marked disagreement with both observed and theoretical behaviors. While it may appear at first sight that the large amplitudes lend credence to the measurements, this conclusion is not supported by closer examination of the data. The large temperature amplitudes do not result from a systematic upward increase of geopotential height amplitudes, as required by the measured temperatures, but rather from erratic variation along the vertical of the phase and amplitude of the computed geopotential height oscillation (see Table 4).

The erratic and implausible behavior of the geopotential height wave stems from the sensitivity of the computations to small errors in the measured wind components when νu and fv are of approximately the same size (near 30N and 30S). For instance, if u and v differ in phase by 90°, it can be seen from Eq. (3) that the phase of the height wave differs by 180° depending upon whether νu is greater than fv or *vice versa*. Since νu and fv are of about the same size in the present experiment and the average phase difference is close to 90°, errors of measurement are probably in themselves sufficient to account for the erratic phase variations. The large, irregular semidiurnal and terdiurnal variations in Table 2b may be cited as evidence that the wind data do indeed contain considerable noise due either to errors of measurement or to real fluctuations of nontidal origin. The conclusion we draw from this exercise is that under ordinary circumstances temperature variations cannot be inferred from wind data in tidal experiments of limited duration. Only by treating many cases statistically can one hope to use the foregoing method to derive reliable estimates of the temperature cycle.

A second possible method for inferring whether the observed or theoretical temperature behavior is more plausible will now be described briefly. In this method, a variant of the previous method, Eq. (3) is rearranged to give the zonal wind variation in terms of the meridional wind and geopotential height variations. The height variations are obtained from the temperature variations by integration of the hydrostatic equation upward from some reference level, here chosen to be 40 km. The resulting equation is

$$u_r = -\nu^{-1}(if v_r + g\eta h_r). \quad (5)$$

The subscripts indicate that the equation is to be applied to relative values of the variables.

The object of this method is to ascertain whether the gross features of the observed zonal wind behavior are in better agreement with the behavior computed from the observed temperatures or the theoretical temperatures. The choice of the meridional component rather than the zonal component as the independent variable was dictated by its more regular behavior.

The results of the computation are presented in Table 5. At lower levels both sets of temperatures give equally good estimates of the relative zonal wind. The similarity at these levels can be traced to the dominance of the term in v_r on the right hand side of Eq. (5). At higher levels both computations yield am-

TABLE 5. Observed zonal wind variation relative to 40 km and variations computed from observed and theoretical temperature variations. Phase gives time of maximum.

Height (km)	Observed Amplitude (m sec^{-1})	Observed Phase (hr)	Computed from observed temperatures Amplitude (m sec^{-1})	Computed from observed temperatures Phase (hr)	Computed from theoretical temperatures Amplitude (m sec^{-1})	Computed from theoretical temperatures Phase (hr)
44	8.8	0.9	7.1	0.2	7.5	0.0
48	15.0	21.5	12.1	20.8	12.1	20.0
52	14.5	18.2	6.2	16.6	9.3	15.9
56	11.0	16.8	6.2	21.3	5.1	16.2
60	10.4	14.2	13.2	21.1	7.7	18.1

plitudes which differ considerably from the observed amplitudes, while the phases determined from the theoretical temperatures more closely resemble the observed phases.

On the basis of these results we must conclude that neither set of temperatures leads to decisively better predictions of the zonal wind behavior, even though at the uppermost level (60 km) the two predictions differ sufficiently to provide a possible basis for favoring one or the other. Conceivably neither set of temperatures is realistic, or alternatively, and perhaps more likely, the harmonic analysis of the zonal wind at the higher levels is distorted by accidental influences and does not depict the true behavior.

As a final means of deciding on the reality of the large observed temperature variations, we consider the possible role of adiabatic heating and cooling in enhancing the temperature cycle derived from radiation theory. Data presented by Webb (1964, 1965) suggest that the meridional wind component varies little over middle latitudes. Thus the assumption will be made that the horizontal velocity divergence is determined solely by the east-west variation of the zonal component. With this assumption the equation of continuity, when integrated between level p and the top of the atmosphere ($p=0$), becomes

$$\omega=-p\frac{\partial\bar{u}}{\partial x}, \tag{6}$$

where $\omega=dp/dt$, the substantial pressure derivative (hereafter referred to as the vertical motion), and the overbar represents a vertical average with respect to pressure. Expressing now the variation of ω by

$$\omega=\hat{W}e^{i(\nu t+\eta x)}, \tag{7}$$

we find that

$$\omega=-i\eta p\bar{u}. \tag{8}$$

The distribution of ω with height computed from Eq. (8) is shown in the left half of Table 6 for two different upper boundary conditions. In case I it is assumed that the net divergence is zero above 60 km so that $\omega=0$ at that level. In case II, the zonal wind variation at 60 km is assumed to persist to the top of the atmosphere. Only at the uppermost levels do these widely different assumptions lead to significantly different vertical velocity estimates.

To compute the temperature variation resulting from the combined effects of diabatic and adiabatic heating, we consider the perturbation form of the thermodynamic energy equation

$$\frac{\partial T'}{\partial t}=\sigma\omega+q, \tag{9}$$

where T' is the perturbed temperature, q is the perturbed diabatic heating rate (in °C per unit time) and

$$\sigma\equiv(1/\rho c_p-\partial T/\partial P). \tag{10}$$

In (10), c_p is the specific heat at constant pressure and ρ and T are standard or unperturbed density and tem-

TABLE 6. Vertical motions derived from horizontal velocity divergence under two different assumptions, and corresponding temperature variations from combined adiabatic and diabatic heating. Phase denotes time of maxima. Case I assumes that the net divergence is zero above 60 km. Case II assumes that the zonal wind variation at 60 km persists to the top of the atmosphere.

Height (km)	Case I Vertical motion Amplitude (10^{-7} mb sec^{-1})	Case I Vertical motion Phase (hr)	Case II Vertical motion Amplitude (10^{-7} mb sec^{-1})	Case II Vertical motion Phase (hr)	Case I Temperature Amplitude (°C)	Case I Temperature Phase (hr)	Case II Temperature Amplitude (°C)	Case II Temperature Phase (hr)
40	9.4	1.7	9.6	23.5	2.2	17.7	2.0	17.3
44	14.8	1.5	14.9	0.1	3.1	17.2	2.8	17.8
48	13.0	23.7	15.7	22.3	2.9	16.3	2.8	15.7
52	8.0	21.7	12.6	20.6	2.4	15.7	2.5	14.1
56	3.1	20.3	8.4	19.5	1.8	16.3	2.1	13.2
60	0.0	—	5.4	18.9	1.8	18.0	1.6	12.3

perature, respectively. Letting

$$\begin{pmatrix} T' \\ q \end{pmatrix} = \begin{pmatrix} \hat{T} \\ \hat{Q} \end{pmatrix} e^{i(\nu t + \eta x)}, \tag{11}$$

Eq. (9) yields

$$T' = -i\nu^{-1}(\sigma\omega + q). \tag{12}$$

Solutions of this equation for the two cases are shown on the right half of Table 6. The diabatic heating rate was obtained by time differentiation of the diurnal temperature wave computed by Leovy (1964)[2]. The solutions reveal that the effect of adiabatic heating is to reduce somewhat the temperature amplitude at the top level and to increase slightly the amplitude at intermediate and lower levels. In both cases the phase of the temperature oscillation is advanced and in case II computed and observed phases are in close accord at most levels. However, computed amplitudes are much smaller than observed, and it appears doubtful that the two can be brought into agreement by any reasonable alteration of the assumptions made in estimating the adiabatic effect.

From this third exercise we conclude that the adiabatic heating and cooling are unable to account for the discrepancy between the observed and theoretical temperature oscillations. Either the temperature measurements must be in error or else radiative or other diabatic effects must be larger than present theory suggests.

5. Conclusions

There is an unmistakable, dominant, diurnal tidal oscillation in the stratopause region over White Sands, New Mexico, during most or all seasons. This motion is most clearly evident in the meridional (v) component. Reed *et al.* (1966) have recently examined all routine rocket observations made at White Sands during June, July, and August through 1964 and found a pronounced diurnal oscillation in the meridional component near the stratopause. A recent additional series of rocket soundings over 48 hours at White Sands on 9, 10 and 11 October 1965, have been found from preliminary analysis to be in close agreement with the June–July series presented here. Considering these cases together with the February (White Sands), May (Eglin, Florida), and November (White Sands) cases reported by Miers (1965), one is led to conclude that the diurnal tide persists throughout the whole year.

The measurements indicate a corresponding diurnal temperature variation with amplitudes as large as 8.2C near the stratopause. This figure is considerably in excess of current theoretical estimates. An attempt to arrive at an independent estimate of the temperature cycle, based essentially on a generalized thermal wind equation, yielded inconclusive results. It was shown that it is unlikely that adiabatic heating as treated here can account for the difference between observed and theoretical temperature variations.

Acknowledgments. We wish to thank Dr. Conway Leovy of the Rand Corporation for providing us with unpublished examples of the diurnal heating cycle in the stratosphere derived from radiative and photochemical theory.

[2] *Loc. cit.*

REFERENCES

Beyers, N. J., and B. T. Miers, 1965: Diurnal temperature change in the atmosphere between 30 and 60 km over White Sands Missile Range. *J. Atmos. Sci.*, **22**, 262–266.

Clark, G. Q., and John G. McCoy, 1965: Measurement of stratospheric temperature. *J. Appl. Meteor.*, **4**, 365–370.

Conrad, V., and L. W. Pollak, 1950: *Methods in Climatology.* 2nd ed., Cambridge, Harvard University Press, 459 pp.

Eddy, Amos, C. E. Duchon, F. M. Haase and D. R. Haragan, 1965: The determination of winds from meteorological rocketsondes. Tech. Report, No. 2, November 1965, Atmos. Science Group, Univ. of Texas, 30 pp.

Harris, M. F., F. G. Finger and S. Teweles, 1962: Diurnal variation of wind, pressure, and temperature in the troposphere and stratosphere over the Azores. *J. Atmos. Sci.*, **19**, 136–149.

Johnson, F. S., 1953: High-altitude diurnal temperature changes due to ozone absorption. *Bull. Amer. Meteor. Soc.*, **34**, 106–110.

Lenhard, R. W., 1963: Variation of hourly winds at 35 to 65 km during one day at Eglin Air Force Base, Florida. *J. Geophys. Res.*, **68**, 227–234.

Leovy, C., 1964: Radiative equilibrium of the mesosphere. *J. Atmos. Sci.*, **21**, 238–248.

Miers, B. T., 1965: Wind oscillations between 30 and 60 km over White Sands Missile Range, New Mexico. *J. Atmos. Sci.*, **22**, 382–387.

Pressman, J., 1955: Diurnal temperature variations in the middle atmosphere. *Bull. Amer. Meteor. Soc.*, **36**, 220–223.

Reed, R. J., D. J. McKenzie and J. C. Vyverberg, 1966: Further evidence of enhanced diurnal tidal motions near the stratopause. *J. Atmos. Sci.*, **23**, 247–251.

Wagner, N. K., 1964: Theoretical accuracy of the meteorological rocketsonde thermistor. *J. Appl. Meteor.*, **3**, 461–469.

Webb, W. L., 1964: Stratospheric solar response. *J. Atmos. Sci.*, **21**, 582–591.

——, 1965: Morphology of noctilucent clouds. *J. Geophys. Res.*, **70**, 4463–4476.